Probes of the Metal-to-Ligand Charge-Transfer Excited States in Ruthenium-Am(m)ine-Bipyridine Complexes: The Effects of NH/ND and CH/CD Isotopic Substitution on the 77 K Luminescence

Yuan-Jang Chen,[†,‡] Puhui Xie,[†] John F. Endicott,*[,†] and Onduru S. Odongo[†]

Department of Chemistry, Wayne State University, Detroit, Michigan 48202, and Department of Chemistry, Fu-Jen Catholic University, 510 Chung Cheng Rd., Hsinchuang, Taipei Hsien 24205, Taiwan, Republic of China

Received: September 29, 2005; In Final Form: March 29, 2006

The effects of ligand perdeuteration on the metal-to-ligand charge-transfer (MLCT) excited-state emission properties at 77 K are described for several $[Ru(L)_4bpy]^{2+}$ complexes in which the emission process is nominally {RuIII,bpy−} → {RuII,bpy}. The perdeuteration of the 2,2′-bipyridine (bpy) ligand is found to increase the zero-point energy differences between the ground states and MLCT excited states by amounts that vary from 0 ± 10 to 70 ± 10 cm^{-1} depending on the ligands L. This indicates that there are some vibrational modes with smaller force constants in the excited states than in the ground states for most of these complexes. These blue shifts increase approximately as the energy difference between the excited and ground states decreases, but they are otherwise not strongly correlated with the number of bipyridine ligands in the complex. Careful comparisons of the $[Ru(L)_4(d_8\text{-bpy})]^{2+}$ and $[Ru(L)_4(h_8\text{-bpy})]^{2+}$ emission spectra are used to resolve the very weak vibronic contributions of the C−H stretching modes as the composite contributions of the corresponding vibrational reorganizational energies. The largest of these, 25 ± 10 cm^{-1}, is found for the complexes with L = py or bpy/2 and smaller when L = NH_3. Perdeuteration of the am(m)ine ligands (NH_3, en, or [14]aneN_4) has no significant effect on the zero-point energy difference, and the contributions of the NH stretching vibrational modes to the emission band shape are too weak to resolve. Ligand perdeuteration does increase the excited-state lifetimes by a factor that is roughly proportional to the excited-state−ground-state energy difference, even though the CH and NH vibrational reorganizational energies are too small for nuclear tunneling involving these modes to dominate the relaxation process. It is proposed that metal−ligand skeletal vibrational modes and configurational mixing between metal-centered, bpy-ligand-centered, and MLCT excited states are important in determining the zero-point energy differences, while a large number of different combinations of relatively low-frequency vibrational modes must contribute to the nonradiative relaxation of the MLCT excited states.

Introduction

The metal-to-ligand charge-transfer (MLCT) excited states of transition metal complexes have long been of interest due to their potential applications as high-energy electron-transfer donors and/or acceptors and as useful models of Marcus inverted region electron-transfer behavior.[1−6] However, transition metal complexes characteristically have a large number of electronic excited states in a relatively small energy region, and configurational mixing among these states often makes it difficult to achieve a detailed understanding of their properties.[7−11] Even in such systems, one expects the changes in properties that are induced by isotopic substitution to be useful as probes of intermediate electronic and molecular structure and reaction pathways.[12] For example, Yersin and co-workers have proposed that the observation of a relatively small (40 cm^{-1}) blue shift of both the absorption and emission band origins following perdeuteration of the $[Ru(bpy)_3]^{2+}$ complex implicates extensive electron delocalization among the three ligands in the metal-to-ligand charge-transfer (MLCT) excited state and that a normal coordinate-based model of the excited state predicts that this blue shift will be approximately 210 cm^{-1} if all of the charge is localized on a single bipyridine (bpy) ligand.[10,13] This suggests that the shifts of the differences in zero-point energies (Δzpe) of the{g,0} ↔ {e,0′} transitions that occur when the bpy ligand is perdeuterated might be a relatively direct experimental measure of the excited-state charge distribution.

In addition to such variations in zpe's, the variations in other spectroscopic features that result from isotopic substitution have often been used to identify the vibrational modes that are coupled to the electronic transitions,[9−11,13−17] and the kinetic responses to isotopic substitution have often proved useful as probes of the pathways for excited-state relaxation.[12,14,18,19] The nearly 2-fold increase of the MLCT excited-state lifetime upon CH/CD isotopic substitution in $[Ru(bpy)_3]^{2+}$,[14,18] or the somewhat larger increase of lifetime upon NH/ND isotopic substitution in $[Ru(NH_3)_4bpy]^{2+}$,[20] might be interpreted in terms of nuclear tunneling mechanisms involving only the highest frequency vibrational modes (C−H or N−H stretching modes, respectively). This is an attractive interpretation because relatively few quanta of excitation in these modes are required to span the ground-state/excited-state energy gap. However, this interpretation requires some distortion of the excited-state structure in the nuclear coordinates of the correlated vibrational

[†] Wayne State University.
[‡] Fu-Jen Catholic University.

10.1021/jp055561x CCC: $33.50
Published on Web 06/06/2006

modes,[21,22] and the accompanying high-frequency vibronic contributions have not been reported in the resonance-Raman spectra of either complex.[14,23] On the other hand, the reported isotope effects may arise from differences in the zpe's, the combined effect of the smaller perturbations of a large number of lower frequency vibrational modes[14] or some combination of these mechanisms. If the isotope effects must be attributed to the combined effect of a large number of relatively low-frequency vibrational modes,[14] then a very large number of relaxation channels are implicated in the excited-state decay (or back electron transfer).[20] This would invalidate single vibrational mode models for this class of Marcus inverted region electron-transfer systems, and any model appropriate for such an electron-transfer process will be correspondingly more complicated.

We have been using a carefully calibrated near-infrared emission spectrometer to critically examine the relatively long wavelength emission spectra of several classes of complexes.[15,20,24,25] The high quality of these emission spectra has enabled us to search for the previously undetected contributions of the high-frequency (C−H or N−H stretching) vibrational modes by examining the differences in the emission spectra of isotopomers[15] and, thereby, to address the relevance of these modes to the excited-state distortions and nonradiative relaxation rates. In this work, we compare the effects of isotopic substitution on the properties of the MLCT excited states for a closely related series of $[Ru(Am)_{6-2n}(bpy)_n]^{2+}$ complexes ($n = 1$, 2, or 3; Am = NH_3 or amine) which have a significant range of excited-state energies. The vibronic parameters inferred from the resonance-Raman spectra[23] in combination with the fundamental component for the {g,0} ↔ {e,0′} transition of the $[Ru(NH_3)_4bpy]^{2+}$ complex have been fitted exceptionally well to the emission spectra obtained in frozen solutions at 77 K by using a Gaussian model for these contributions: the band shape is reproduced very accurately and the amplitude of the observed envelope of vibronic contributions is about 10% smaller than that calculated;[20] this is illustrated in Figure S1.[26] In general, we base the analysis of emission band shapes on the progressions of vibrational modes that correspond to the displacements in those nuclear coordinates that describe the differences in ground- and excited-state molecular geometries. The comparisons of the band shapes of this series of complexes are complicated by the very large electronic matrix elements associated with the allowed MLCT transitions in these complexes ($H_{ge} \cong 7000$ cm^{-1} for bpy;[27] similar values of H_{ge} and values of $H_{eg} \geq {}^1/_3 H_{ge}$ have been obtained from Stark spectroscopy of closely related complexes[28]) and the resulting configurational mixing between the ground (g) and excited (e) states, where the mixing coefficient is $\alpha_{ge} \cong (H_{ge}/h\nu_{max(abs)})/[1 + (H_{ge}/h\nu_{max(abs)})^2]^{1/2}$; this is qualitatively illustrated in Figure 1. One experimentally observable effect of this configurational mixing is the attenuation of the vibronic sideband components of the emission spectra as the excited-state energy decreases (i.e., as n decreases from 3 to 1).[24] The complications that result from this configurational mixing can usually be addressed by means of perturbation-theory-based arguments. The comparisons are further complicated if there are differences in bandwidth among the complexes, and corrections for this can be based on modeling of the variations in observable parameters[20] using the resonance-Raman parameters reported for $[Ru(bpy)_3]^{2+}$ [14] and $[Ru(NH_3)_4bpy]^{2+}$.[23] The work described here indicates that the differences of Δzpe between the CH and CD isotopomers, ∇zpe = [Δzpe(CD) − Δzpe(CH)], of mono-bpy complexes vary from about zero to at least twice the value reported for $[Ru(bpy)_3]^{2+}$,[10] and it establishes that the excited-state displacements in the high-frequency C−H and N−H stretching modes are too small to dominate the nonradiative relaxation channels of Ru/bpy ^{3}MLCT excited states.

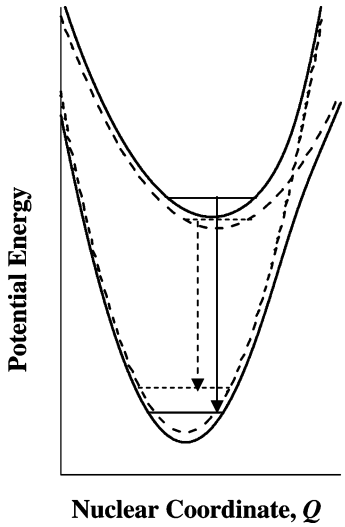

Figure 1. Qualitative potential energy curves that illustrate the effects of configurational mixing when the force constant of the excited state is less than that of the ground state. Dashed lines for the diabatic curves and the {e,0′} → {g,0} transition between them; solid lines for the adiabatic curves and the transition between them. Configurational mixing of the two states increases the difference in energy between them by $2\epsilon_s$ and it increases the zpe of the excited state while decreasing that of the ground state.

Experimental Section

A. Materials. The ligands 2,2′-bipyridine (bpy) and ethylenediamine (en) were purchased from Aldrich and used without further purification. The [14]aneN$_4$ ligand ([14]aneN$_4$ = cyclam = 1,4,8,11-tetraazacyclotetradecane), was synthesized according to literature procedure.[29] The perdeuterated ligand d_8-2,2′-bipyridine (d_8-bpy) was purchased from the Aldrich Chemical Co.

The complexes $RuCl_3 \cdot xH_2O$ ($x \leq 1$), *cis*-$Ru(bpy)_2Cl_2$, and $[Ru(NH_3)_5Cl]Cl_2$ were purchased from Strem Chemicals and used as received; $[Ru(bpy)_3]Cl_2$, also purchased from Strem Chemicals, was recrystallized before use. The complexes $[Ru(NH_3)_5(O_3SCF_3)](O_3SCF_3)_2$,[30] $[Ru(NH_3)_4bpy](PF_6)_2$,[31−33] $[Ru(NH_3)_2(bpy)_2](PF_6)_2$,[31−33] $[Ru(bpy)Cl_4]$,[34] $[Ru(en)(bpy)_2](PF_6)_2$,[35] $[Ru(bpy)_2(O_3SCF_3)_2]$,[30] and $[Ru([14]aneN_4)bpy](PF_6)_2$[36] were prepared and characterized by slight modifications of literature procedures as described elsewhere.[20] Professor James R. Kincaid provided the initial sample of $[Ru(d_8\text{-bpy})_3]Cl_2$. Other inorganic reagents were reagent grade, organic solvents were spectral grade, and water was deionized and distilled.

Am(m)ine deuterated complexes were prepared by dissolving the corresponding proteo-complex in D_2O and then precipitating it by adding saturated $NaPF_6/D_2O$ solution to the mixture. This procedure was repeated several times as described previously.[15,37,38] The $[Ru(NH_3)_{6-2n}(d_8\text{-bpy})_n]^{2+}$ complexes were prepared by the standard procedures referenced above. The am(m)ine and bpy perdeuterated complexes were characterized by IR spectra and by ^{1}H NMR. In addition, the quality of the perdeuteration procedure is illustrated by the clean separation of isotopomer vibronic components as illustrated in Figure 2.

B. Instrumentation. Routine emission spectra at room temperature in the 500−800 nm range were recorded on a SPEX Fluorolog instrument and corrected for instrument response with the correction file packaged with the instrument's software or

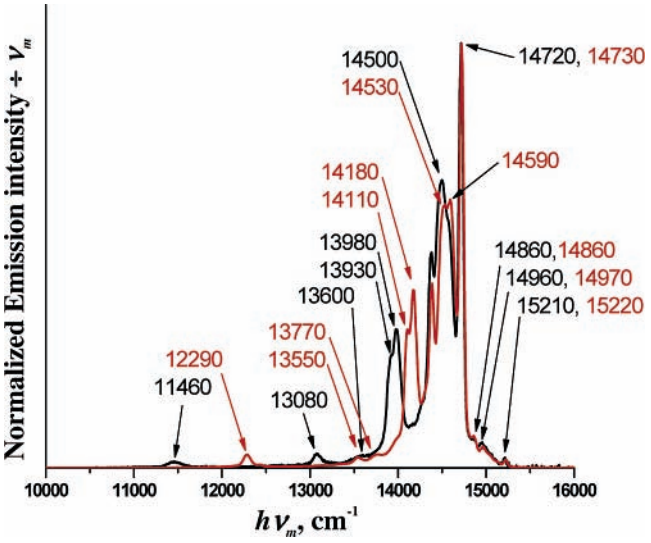

Figure 2. Emission spectra of $[Cr(NH_3)_5CN](PF_6)_2$ (black) and $[Cr(ND_3)_5CN](PF_6)_2$ (red) determined at 77 K in DMSO/H_2O and DMSO/D_2O, respectively. The origin ($E^{0'0}$) of the emission bands, at 14 720 and 14 730 cm^{-1}, respectively, and the peak energies of the vibronic components are identified in the figure. On the basis of the isotope induced frequency shifts, the $[Cr(NH_3)_5CN](PF_6)_2$ peaks at 11 460, 13 080, and 13 930−13 990 are assigned as N−H stretching, NH_2 deformational, and Cr−N−H rocking vibrations, respectively; the peaks observed for these vibrations are the result of the convolution of the contributions from several vibrational modes in each case.

on a SPEX Tau-2 instrument (500−850 nm range) with DataMax software. Routine UV−vis spectra were recorded using a Shimadzu UV-2101PC spectrophotometer. For emission spectra in wavelength regions longer than 850 nm, we used a Princeton Instruments (Roper Scientific) OMAV/InGaAS array detector mounted on an Acton SP500 spectrometer. Details of the procedures used are presented elsewhere.[15,20] The intensity responses of the Tau2 and InGaAs-based spectrometers were calibrated with respect to the intensity output of an Oriel Model 63358 Quartz Tungsten Halogen lamp with NIST traceable calibrated intensity output. The wavelength response of the InGaAs spectrometer was calibrated with respect to the Xe emission lines of an Oriel Spectral Calibration lamp (model 6033). Samples were prepared by dissolving the complexes in butyronitrile, DMSO/H_2O (1:1) or DMSO/D_2O (1:1) and transferring the solutions to 2 mm i.d. cylindrical luminescence cells. Glasses for the spectroscopic measurements were prepared by immersing these cells in a liquid nitrogen bath in a quartz Dewar secured with a Derlin holder. Only samples that formed good clear glasses were used in this study. Emission data from the InGaAs spectrometer were collected using the WinSpec program. The sample cell and Dewar were aligned for each experiment to optimize the signal. Optical filters were used to reduce the scattered laser light. Spectra were accumulated for several independently prepared samples and for different preparations for each complex. The sample spectra reported here are the averages of 20−40 spectral scans of two or three independently prepared samples.

Luminescence lifetimes were determined by using a PRA LN 1000 nitrogen laser-pumped PRA LN 107 dye laser for sample excitation and passing the emitted light through an ISA H-100 monochromator to a Hammamatsu 950 PMT (photomultiplier tube). The PMT was coupled to a LeCroy 9310 digital oscilloscope and interfaced to a computer.[10] Software for this system was written by OLIS, Inc. (Jefferson, GA).

C. Data Analysis Procedures. 1. General. The procedures that we used are described in detail elsewhere.[15,20] The emission intensity at a frequency ν_m can be represented in general form as[39−42]

$$I_{\nu_m} = \frac{64\pi^4}{3h^3c^3 \ln 10} \frac{\nu_m \eta^3 H_{eg}{}^2 (\Delta\mu_{eg})^2}{(4\pi\lambda_s k_B T)^{1/2}} (\mathrm{FC}) \qquad (1)$$

where η is the index of refraction, ν_m is the frequency of the incident radiation, $H_{eg}\Delta\mu_{eg}/h\nu_m$ has been substituted for the transition dipole, M_{eg},[41−43] H_{eg} is the electronic matrix element, $\Delta\mu_{eg}$ is the difference between excited-state and ground-state dipole moments, λ_s is the solvational reorganizational energy, and c is the speed of light. On the basis of Gaussian band shapes and a wave packet model and for the contributions of a single vibrational mode, (FC) can be represented by[39−41]

$$(\mathrm{FC}) = \sum_j F_{j,h}[e^{-\{4G_j{}^2 \ln 2/\Delta\nu_{1/2}{}^2\}}] \qquad (2)$$

$$F_{j,h} = \frac{S_h{}^j e^{-S_h}}{j!} \qquad (3)$$

$$S_h = \lambda_h/h\nu_h$$

$$G_j = E^{0'0} - \lambda_s - jh\nu_h - h\nu_m \qquad (4)$$

We transferred the ASCII files for the observed spectra to Excel, and further analysis was based on a Gaussian model for the contributions of the fundamental and vibronic components to the observed emission spectrum.[7,20] The differences in zero-point energies, $E_{ge}^{0'0}$, and the low-frequency reorganizational energy contributions, λ_s, which are associated with the redistribution of charge, are difficult to determine independently from the emission spectra of species in solution. To evaluate the emission spectra in terms of the experimentally accessible parameters, we use (i) the full width at half-height, $\Delta\nu_{1/2}$, rather than λ_s and (ii) the energy of the maximum of the fundamental component of the emission spectrum, $h\nu_{max(f)} = E_{ge}^{0'0} - \lambda_s$, rather than $E_{ge}^{0'0}$. We determine the fundamental ($j = 0$) for the $\{e,0'\} \rightarrow \{g,0\}$ transition from the experimental spectrum as a Gaussian function, $I_{\nu_{m(f)}}$, with maximum intensity $I_{max(f)}$ at a frequency of $\nu_{max(f)}$ and full width at half-height of $\Delta\nu_{1/2}$ (the deconvolution procedure is described elsewhere[20,27] and summarized below). The intensity of the fundamental at a frequency ν_m is then

$$I_{\nu_m(f)} \cong I_{max(f)} e^{-\{[h\nu_{max(f)} - h\nu_m]^2/(\Delta\nu_{1/2}{}^2/4\ln 2)\}} \qquad (5)$$

1. Evaluation of the Fundamental Component of the Emission Band. First, the observed spectral intensities were divided by the emission energy (see eq 1) and the intensity of the maximum of the resulting spectrum was adjusted to 1.00 using EXCEL. The resulting spectral data were then transferred to Grams-32 for deconvolution of the Gaussian function representing the fundamental. The Gaussian fits were constructed so that $I_{\nu_{m(f)}}$ matched the slope on the high-energy side of the experimental emission as closely as possible while accounting for most of the intensity of the high-energy feature.[15,20,27,44] This procedure is based on the representation of the emission spectra as summations over Gaussian functions corresponding to the fundamental ($j = 0$) and vibronic progressions in the distortion modes.[39−41,45,46] The 512 pixel InGaAs array-based spectrometer was configured so that the 512 pixels of the detector approximately span a 75 nm spectral window. This results in approximately 0.2 nm or 0.3% uncertainty in

the wavelength determined in each spectral scan. The corresponding uncertainties in the energy determinations per scan of the $[Ru(bpy)_3]^{2+}$ and $[Ru(NH_3)_4bpy]^{2+}$ emissions are approximately 35 and 25 cm^{-1}, respectively. We have reduced the former to about 18 cm^{-1} by using second-order scattering from the spectrometer in our energy determinations of $[Ru(bpy)_3]^{2+}$, and this intrinsic source of uncertainty was further reduced to less than about 7 cm^{-1} by using the average of 20−40 spectral scans for each spectral determination.

2. Vibronic Contributions to the Emission Spectra in Frozen Solution. When the distortions (a_h) in the vibrational modes that correlate with the difference in excited-state and ground-state geometry are small ($\lambda_h/h\nu_h \leq 0.1$, where $\lambda_h = {}^1/_2 f_h (a_h)^2$ is the vibrational reorganizational energy for the hth vibrational mode), the first-order vibronic progressions can be organized into the respective first-order, $I_{\nu_m(0'1)}$, second-order, $I_{\nu_m(0'2)}$, third-order, $I_{\nu_m(0'3)}$, etc. Gaussian contributions,[7,20] and the intensity at a frequency ν_m, can be calculated from these components if resonance-Raman (rR) data are available[20]

$$I_{\nu_m(\mathrm{calcd})} \cong I_{\nu_m(\mathrm{f})} + I_{\nu_m(0'1)} + I_{\nu_m(0'2)} + I_{\nu_m(0'3)} + \ldots \quad (6)$$

3. Empirical Reorganizational Energy Profiles (emrep's) and the Search for High-Frequency Vibronic Contributions. The intensity of a first-order vibronic contribution to the emission spectrum (i.e., for any one term, $h\nu_h$, contributing to eq 6) is given by[47,48]

$$I_{\max(h)} = \left(\frac{\lambda_h}{h\nu_h}\right) I_{\max(f)} \quad (7)$$

In principle, a difference spectrum constructed as $I_{\nu_m(\mathrm{diff})} = I_{\nu_m(\mathrm{expt})} - I_{\nu_m(\mathrm{fit})}$ corresponds to the envelope of vibronic contributions to the emission spectrum; however, vibronic contributions with very large $h\nu_h$ (e.g., 2800−3200 cm^{-1} for C−H and N−H stretching frequencies) necessarily have very small values or $I_{\max(h)}$. This has led us to construct emrep's to facilitate the search for these high-frequency contributions.[7,15,20] The emrep's are based on solving eq 7 for λ_h; they are generated by multiplying the experimental difference spectrum by $h\nu_d = h(\nu_{\max(f)} - \nu_m)$ or

$$\Lambda_m = h\nu_d \left(\frac{I_{\nu_m(\mathrm{diff})}}{I_{\max(f)}}\right) \quad (8)$$

where in principle, $I_{\nu_m(\mathrm{diff})} = [I_{\nu_m(0'1)} + I_{\nu_m(0'2)} + I_{\nu_m(0'3)} + \ldots]$. Since the functions contributing to Λ_m have significant bandwidths but are not Gaussian functions, the maxima in the corresponding spectral representation (Λ_m vs ν_d) will not occur at the correct vibrational frequencies (ν_h). We make an approximate correction for this bandwidth effect, based on the first-order vibronic terms, by substituting $h\nu_x = 2(h\nu_d) - [(h\nu_d)^2 + (\Delta\nu_{1/2})^2/4 \ln 2]^{1/2}$ for $h\nu_d$ in eq 8 so that the reorganizational energy profile is given by a plot of Λ_x vs $h\nu_x$,[7,15,20] where

$$\Lambda_x = h\nu_x \left(\frac{I_{\nu_m(\mathrm{diff})}}{I_{\max(f)}}\right) \quad (9)$$

We have previously examined the implications of this procedure[20] based on a Gaussian model for the vibronic components, eq 9, and the rR parameters reported for $[Ru(NH_3)_4bpy]^{2+}$ [23] and $[Ru(bpy)_3]^{2+}$.[14]

In this report, we use emrep's in the search for the contributions from the highest frequency vibrational modes. The approach that we use is based on the differences in the emrep's of the respective isotopomers, that is, $[\Lambda_{x(RH)} - \Lambda_{x(RD)}]$ vs $h\nu_x$ (R = C or N).[15] However, the component bandwidths are a major factor contributing to the amplitudes of the emrep's,[20] and corrections for the effects of differences in bandwidths must be made for some interpretations of these quantities.

4. Corrections. The bandwidths found for charge-transfer emissions in 77 K frozen solutions are large ($\Delta\nu_{1/2}$ = 600−1100 cm^{-1}), and our Grams32 deconvolution procedure inevitably includes some or all of the contributions of vibrational modes for which $(h\nu_{\max(f)} - h\nu_h) < \sim\Delta\nu_{1/2}$ into our evaluation of the fundamental. As a result, the spectrum calculated with the fundamental obtained from this deconvolution of the observed spectra and the rR components is 10−30% too intense (note that we normalize the observed intensity maxima to unity). Thus, corrections for the differences in bandwidth must be made to compare the variations in spectroscopic parameters of a series of complexes. Similarly, all the parameters of interest, including the observed bandwidth and energy of the deconvoluted fundamental, can be represented as functions of the intrinsic bandwidth, $\Delta\nu_{1/2}$.[20] The necessary corrections are readily generated when rR parameters are available.[20] Since such data are not available for most of the complexes that we have employed, we have used the corrections based on the rR parameters reported for the $[Ru(NH_3)_4bpy]^{2+}$ [23] and/or $[Ru(bpy)_3]^{2+}$ [14] complexes[20] which bracket the range of bandwidths for the complexes reported here.

a. Energy of the Fundamental. The differences between the values of $h\nu_{\max(fit)}$ obtained by the Grams32 deconvolutions and the corresponding zpe's are a function of the component bandwidth. The modeling with the reported rR parameters[20] suggests that the corrections can be expressed as a cubic function of the bandwidth of the deconvoluted fundamental (see the Supporting Information).[26] Correcting for the small differences between the bandwidths of the different complexes used in this study can be accomplished with simple linear functions of $\Delta\nu_{1/2(fit)}$. Thus, for $[Ru(NH_3)_4bpy]^{2+}$ and $[Ru(bpy)_3]^{2+}$, respectively

$$h\nu_{\max(fit)} \cong 17276 - 0.09785\Delta\nu_{1/2(fit)} \quad (10)$$

$$h\nu_{\max(fit)} \cong 12561 - 0.1316\Delta\nu_{1/2(fit)} \quad (11)$$

The extrapolation to $\Delta\nu_{1/2(fit)} = 0$ is possible in principle, but the uncertainties that accompany the extrapolation are considerable, and we have corrected $h\nu_{\max(fit)}$ to the narrowest observed bandwidth for our comparisons. As a result, $h\nu_{\max(fit)}$ contains some reorganizational energy contributions from low-energy vibrational modes for which $h\nu_i < \sim\Delta\nu_{1/2(corr)}$, so that $h\nu_{\max(fit)} = \Delta\mathrm{zpe} - \lambda_s$. If these contributions are the same in the isotopomers, then their differences in $h\nu_{\max(f;corr)}$ will correspond to the differences in ∇zpe. The small shifts in low-frequency vibrational modes that result from perdeuteration of the ligands may result in small systematic errors in the evaluation of ∇zpe for the deutereo- and proteo-isotopomers. However, the values of λ_s are small ($\leq \sim 5\% \times h\nu_{\max(f)}$ if they are the only contributions to $\Delta\nu_{1/2}$) and they may be unimportant in frozen solutions, so systematic variations in the values of λ_s are not likely to be important in the evaluations of ∇zpe.

b. Bandwidth Corrections for emrep's. We assume that the second- and third-order reorganizational energy contributions of the vibrational modes are very weakly dependent on isotopic substitution and that the important bandwidth corrections of the differences in the emrep's in the high-frequency regimes ($h\nu_x$ > 2000 cm^{-1}) of the isotopomers can be based on the first-

TABLE 1: Spectroscopic Parameters for $[Ru(Am)_{6-2n}(bpy)_n]^{2+}$ Complexes[a]

ligands	$h\nu_{abs(max)}$ (solvent)[b]	$h\nu_{em(max)}$, 298 K	$h\nu_{em(max)}$, 77 K	$h\nu_{f(max)}$, [$\Delta\nu_{1/2}$], 77 K {$h\nu_{f(max)}$, [$\Delta\nu_{1/2}$], 298 K}	$\Lambda_x(\nu_x)$, 77 K
$(bpy)_3$	21.9(d/w)	15.98	17.12	17.22 [0.68] {16.53[1.64]}	1.16(1.49)
	22.12(bun)	16.2	17.24	17.31[0.64]	1.05(1.50)
$(en)(bpy)_2$	20.2(d/w)	13.9	15.00	15.06[0.78]	1.00(1.50)
	20.4(bun)	14.35	15.26	15.28[0.80]	0.88(1.49)
$(NH_3)_2(bpy)_2$	20.4(d/w)	13.52	14.56	14.64[0.91]	0.99(1.53)
	20.2(bun)	13.98	14.67	14.70[0.78]	0.86(1.49)
$(py)_4bpy$	22.6(bun)		16.85	16.87[0.81]	0.87(1.40)
$([14]aneN_4)(bpy)$	19.0(d/w)	12.94	13.96	14.01[0.95]	0.85(1.44)
	19.5(bun)	13.38	13.99	14.03[0.89]	0.81(1.45)
$(en)_2(bpy)$	19.1(d/w)	11.81	12.82	12.88[1.03]	0.85(1.45)
	19.2(bun)	12.59	13.01	13.05[0.89]	0.78(1.45)
$(NH_3)_4(bpy)$	18.8(d/w)		12.02	12.09[1.11]	0.81(1.45)
	19.0(bun)		12.37	12.42[0.92]	0.80(1.48)
$(d_8\text{-bpy})_3$	22.15(bun)		17.27	17.34[0.64]	1.06(1.51)
$(en)(d_8\text{-bpy})_2$	20.5(bun)		15.28	15.32[0.89]	
$(py)_4(d_8\text{-bpy})$	22.6(bun)		16.85	16.87[0.81]	0.86(1.42)

[a] All energies in units of $cm^{-1}/10^3$. [b] Solvent abbreviations: d/w = DMSO/water; bun = butyronitrile. [c] DMSO/D_2O. [d] Trace amounts of H_2O may have been present.

order contributions; thus, for the amplitudes of the emrep maxima at about 1500 cm^{-1} in butyronitrile for $[Ru(NH_3)_4bpy]^{2+}$ ($\Lambda_{1st} = 570\ cm^{-1}$) and $[Ru(bpy)_3]^{2+}$ ($\Lambda_{1st} = 970\ cm^{-1}$)[20]

$$\frac{\partial\Lambda_{1st}}{\partial\Delta\nu_{1/2}} \cong 0.33 \tag{12}$$

where we assume that

$$\Lambda_x = \Lambda_{1st} + \Lambda_{2nd} + \Lambda_{3rd} ... = h\nu_x(I_{\nu_m(0'1)} + I_{\nu_m(0'2)} + I_{\nu_m(0'3)} + ...) \tag{13}$$

and

$$\Lambda_{x(NH)} - \Lambda_{x(ND)} \cong h\nu_x[I_{\nu_m(0'1)}(NH) - I_{\nu_m(0'1)}(ND)] \tag{14}$$

Equation 12 implies a bandwidth correction of about ($5.8 \times 10^{-4} \times \partial\Delta\nu_{1/2}$) in Λ_{1st} for the $[Ru(NH_3)_4bpy]^{2+}$ emrep's. It is important to note that the vibrational reorganizational energy inferred from the rR data for the vibrational modes with a frequency of about 1490 cm^{-1} is 224[23] and 397[14] cm^{-1} for $[Ru(NH_3)_4bpy]^{2+}$ and $[Ru(bpy)_3]^{2+}$, respectively, and that the first-order components contribute only 71% and 89%, respectively, to the total emrep intensities near $h\nu_x \approx 1500\ cm^{-1}$, with the remaining contributions to amplitude arising from overlapping second order and other contributions.[20] Thus, more than half of the amplitude of the corresponding first-order emrep's is a consequence of the finite bandwidths of the components and the significant number of vibronic components with energies of about ($1490 \pm \Delta\nu_{1/2}$) cm^{-1}.

c. Attenuation of emrep's. The vibrational reorganizational energies of a series of complexes are expected to decrease as emission energies decrease as a consequence of their differences in ground-state/excited-state configurational mixing,[27,49-51] and there should be a corresponding decrease in the amplitudes of the vibronic sidebands that correlate with distortions in the high-frequency modes and of the emrep's consistent with the observations on the $[Ru(Am)_{6-2n}(bpy)_n]^{2+}$ complexes.[20,24] For a spin forbidden emission, one expects that $\alpha_{eg} < \alpha_{ge}$ for the normalized mixing coefficients; for $\alpha_{ge} < 0.1$[20,51]

$$\Lambda_k \cong \Lambda_k^\circ(1 - 2\alpha_{ge}^2 - 2\alpha_{eg}^2 + ...) = \Lambda_k^\circ(1 - n_e\alpha_{eff}^2) \tag{15}$$

Correlations of vibronic contributions resolved from frozen solution emission spectra can be based on $\Lambda_k^\circ(1 - n_e\alpha_{eff}^2)$, and the parameters based on observations for the complexes discussed here are summarized in Table S1[26] and discussed elsewhere.[20] The values found for $n_e\alpha_{eff}^2$ vary from 0.3 for $[Ru(bpy)_3]^{2+}$ to 0.7 for $[Ru(NH_3)_4bpy]^{2+}$.[20] In addition, the amplitudes of the emrep's will increase as $\Delta\nu_{1/2}$ increases.[20]

Results

The issues raised by isotopic substitution require very good spectroscopic resolution, and we have addressed this by careful instrumental calibration and the averaging of a large number of individual spectra. As a check on our procedures, we have also examined the emission spectra of $[Cr(NH_3)_5CN](PF_6)_2$ and $[Cr(ND_3)_5CN](PF_6)_2$ (see Ryu et al.[37] and Lessard et al.[38] and the references therein) using the same conditions, techniques, and procedures employed for the $[Ru(Am)_{6-2n}(bpy)_n]^{2+}$ complexes in this study. The spectra of these complexes are shown in Figure 2, and the following features are to be noted: (1) the 0′0 bandwidths of the emissions are limited by our instrumental resolution; (2) the differences in $E^{0'0}$ for the two complexes (10 cm^{-1}) indicate that our estimates of the uncertainties of our energy determinations are reasonably conservative; (3) the vibronic contribution of the high-frequency N−H stretching vibrations (not previously reported) is weak but readily resolved at 11 460 cm^{-1} (this "band" is relatively broad because it is the convolution of the contributions of the 15 N−H stretching vibrations).

Isotopic substitution alters the values of the basic spectroscopic parameters as summarized in Tables 1 and 2. The effect of perdeuteration of the bpy ligand on the spectra and on the emrep's of $[Ru(NH_3)_4bpy]^{2+}$ is illustrated in Figure 3 and also in Figure S2.[26] Perdeuteration of the bpy ligands results in significant shifts of the observed emission band maxima of the $[Ru(Am)_{6-2n}(bpy)_n]^{2+}$ complexes as shown in Figure 4 and in Tables 1 and 2. These shifts correspond to $\Delta h\nu_{max(f)}$ differences in butyronitrile of 30 cm^{-1} for $[Ru(bpy)_3]^{2+}$ and 50−70 cm^{-1} for $[Ru(Am)_4bpy]^{2+}$. The corrections of $\Delta h\nu_{max(f)}$ for the bandwidth differences of $[Ru(bpy)_3]^{2+}$ and the $[Ru(Am)_4bpy]^{2+}$ complexes are small, 3−4 cm^{-1} (based on eqs 10 and 11), and the corrected values ($\Delta h\nu_{max(f)} = 46$ and 67 cm^{-1}, respectively, for $(Am)_4$ = [14]aneN$_4$ and $(NH_3)_4$) are within the limits of experimental uncertainties. In contrast, we were unable to detect any differences in the emission maxima of the isotopomers of $[Ru(py)_4bpy]^{2+}$.

TABLE 2: Effects of Ligand Deuteration on Spectroscopic Properties and Lifetimes of $[Ru(Am)_{6-2n}(bpy)_n]^{2+}$ Complexes

$[Ru(L)]^{2+}$ ligands	$\Delta h\nu_{f(max)}$,[b] cm^{-1}	$\Delta\Lambda_{x(max;N)}$[c] $[h\nu_x]$,[d] cm^{-1} (d/w)[a]	$\Delta\Lambda_{x(max;C)}$[e] $[h\nu_x]$,[d] cm^{-1} (bun)[a]	k_{nr},77 K {k_{nr}, 298 K}, μs^{-1} (solvent)[a]
$(bpy)_3$			20 ± 8[2800]	0.23{1.1} (d/w)
	30 ± 10		-30 ± 1[2100]	0.13{4.3} (bun)
	(CD−CH)			
$(d_8\text{-bpy})_3$			20 ± 1[1200]	0.10{4.3} (bun)
			-25 ± 1[700]	
$(en)(bpy)_2$	35 ± 15	8 ± 1[2600]		1.3{12.3}(d/w)
$(en)(d_8\text{-bpy})_2$	(CH−CD)	-8 ± 1[1900]		0.69{10.2}(bun)
$(d_4\text{-en})(bpy)_2$	20 ± 10	8 ± 1[1900]		0.66{6.2} (d/w) [f]
	(ND−NH)	-9 ± 1[600]		0.41{9.0} (bun)[g]
$(NH_3)_2(bpy)_2$		7 ± 1[2900]		2.9{25) (d/w)
	20 ± 10	-7 ± 1[1950]		1.7{14.5}(bun)
$(ND_3)_2(bpy)_2$	(ND−NH)	8 ± 1[1300]		1.3{13.7}(d/w)[f]
		-6 ± 1[500]		1.1{13}(bun) [g]
$(py)_4bpy$			30 ± 10[2600]	0.15 (bun)
			-10 ± 5[2100]	
$(py)_4(d_8\text{-bpy})$			30 ± 10[1100]	0.12 (bun)
			-15 ± 10[600]	
$(d_5\text{-py})_4bpy$				0.13 (bun)
$([14]aneN_4)bpy$			14 ± 2[2600]	1.59{22.8} (d/w)
	50 ± 10		-14 ± 1[1700]	0.975{19.0}(bun)
$([14]aneN_4)(d_8\text{-bpy})$	(CD−CH)		10 ± 1[1100]	0.52{14}(bun)
			-10 ± 1[600]	
$(en)_2bpy$		5 ± 2[3800]		26(d/w)
	10 ± 10	-8 ± 1[2100]		9.5(bun)
$(d_4\text{-en})_2bpy$	(ND−NH)	15 ± 1[1200]		8.4(d/w) [f]
				5.1{41} (bun) [g]
$(NH_3)_4bpy$		10 ± 5[3300]	15 ± 1[2700]	39(d/w)
	70 ± 10	-10 ± 3[2300]	-15 ± 1[1900]	22(bun)
$(ND_3)_4bpy$	(C −CH)	15 ± 3[1400]	15 ± 1[1200]	13(d/w) [f]
	10 ± 10 cm^{-1}		-15 ± 1[500]	5.1{41}(bun) [g]
$(NH_3)_4(d_8\text{-bpy})$	(ND − NH)			15(bun)

[a] Solvent abbreviations: d/w = DMSO/H_2O except as noted; bun = butyronitrile. [b] $\Delta h\nu_{f(max)} = h\nu_{f(max)}(RD) - h\nu_{f(max)}(RH)$; data from Table 1. [c] $\Delta\Lambda_{x(max;N)} = \Lambda_{x(max;NH)} - \Lambda_{x(max;ND)}$. [d] ν_x = high-frequency maximum amplitude of the emrep difference. [e] $\Delta\Lambda_{x(max;C)} = \Lambda_{x(CH)} - \Lambda_{x(CD)}$. [f] d/w = DMSO/$D_2O$. [g] Trace amounts of H_2O may have been present.

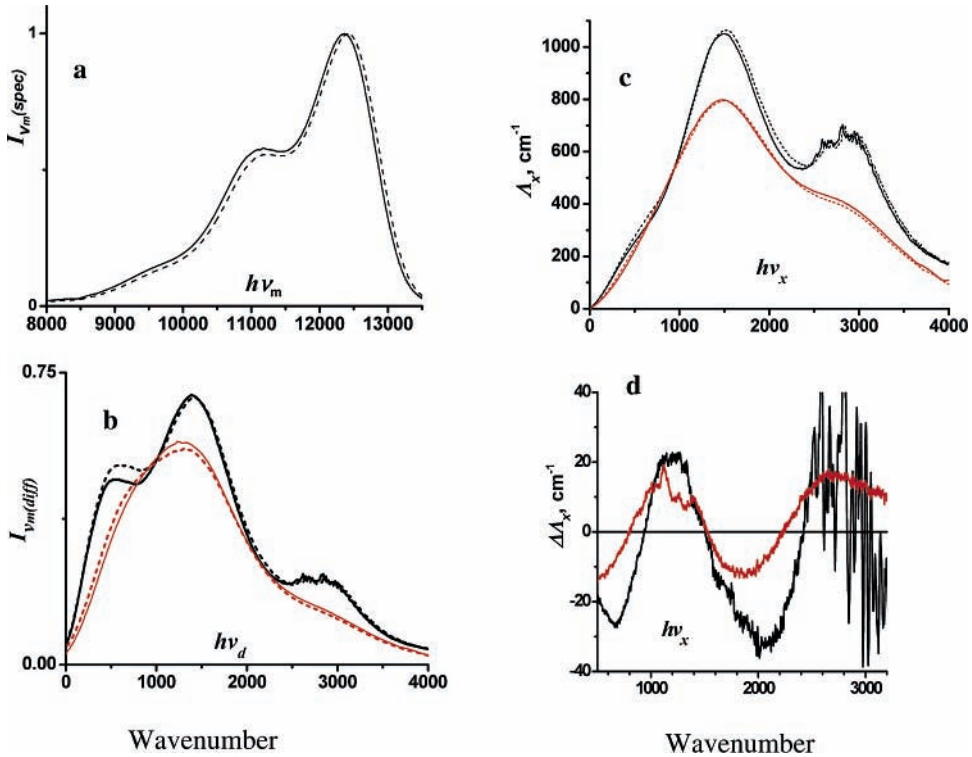

Figure 3. Emission spectra (a), difference spectra (b), emrep's (c), and emrep differences (d) for the $[Ru(bpy)_3]^{2+}$ and $[Ru(d_8\text{-bpy})_3]^{2+}$ isotopomers, black, and the $[Ru(NH_3)_4bpy]^{2+}$ and $[Ru(NH_3)_4(d_8\text{-bpy})]^{2+}$ isotopomers, red; solid lines for bpy and dashed lines for d_8-bpy complexes in a−c.

The apparent blue shifts of the fundamental that result from the perdeuteration of am(m)ine ligands of the tetraam(m)ine complexes are very small and too close to our detection limits (about 10 cm^{-1}) to be reliable; the blue shifts for the diaam-

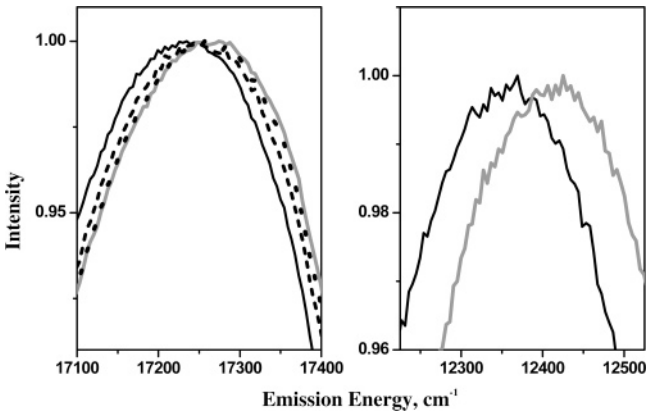

Figure 4. Variations in the energies of the emission maxima of the d_8-bpy (gray lines) and h_8-bpy (black lines) isotopomers of $[Ru(bpy)_3]^{2+}$, top, and $[Ru(NH_3)_4bpy]^{2+}$, bottom. The spectra were obtained in butyronitrile solutions at 77 K and normalized to unit intensity. An energy range of 300 cm^{-1} centered on the emission maximum is displayed in each panel. The percentage of $[Ru(d_8\text{-bpy})_3]^{2+}$ in the butyronitrile solutions is from left to right in the top panel: 0 (solid black), 33 (black dashes), 50 (black dots), and 100 (gray).

(m)ines are slightly larger (about 20 cm^{-1}). On the other hand, perdeuteration of either the am(m)ine or the bpy ligands does increase the lifetimes of the corresponding MLCT excited states. These isotope effects are small but reproducible and statistically significant. The observations are summarized in Table 2.

We have been able to detect very weak, but well-resolved, high-frequency C−H vibronic components in most of the complexes; for an example, see Figure 3. In contrast, the apparent N−H contributions (at about 3000 cm^{-1}) are not significant compared with the signal-to-noise limitations of our data. The plots of $\Delta\Lambda_{x(RH)} = [\Lambda_{x(RH)} - \Lambda_{x(RD)}]$ vs $h\nu_x$, as illustrated in Figures 3 and S2,[26] have reasonably well-defined peaks of alternating positive and negative amplitudes in the range of $h\nu_x$ expected for R = C but not for R = N stretching frequencies. Furthermore, the ratio of $h\nu_{x(max)}$, for the positive peak energy maxima, to $h\nu_{x(min)}$, the peak minima (i.e., for $\Delta\Lambda_{x(RH)} < 0$), for R = C is approximately $(2)^{1/2}$, as expected. The evaluation of the apparent peaks with $h\nu_{x(max)} < \sim 2000$ cm^{-1} is complicated by the sums of the effects of deuteration on the lower frequency bpy skeletal modes. The apparent peaks at about 1000 ± 200 cm^{-1} in the plots of $\Delta\Lambda_{x(CH)}$ vs $h\nu_x$ may correspond to a CH−bpy vibrational mode (or modes) reported at about 1000 cm^{-1}.[52] As discussed elsewhere,[20] the uncertainties in Λ_x become very large below about 500 cm^{-1} where $I_{\nu_m(expt)}$ is roughly comparable with $I_{\nu_m(f)}$. While the profile differences in Figures 3 and S2 demonstrate that there are high-frequency C−H stretching mode contributions to the emission spectra, the amplitudes of the $\Lambda_{x(CH)}$ are very small ($\Delta\Lambda_{x(CH)} \approx 10-20$ cm^{-1} for $\nu_x \cong 2600-2900$ cm^{-1}) and they are only resolvable by averaging many (20 or more) very good spectra. We have estimated the maxima and minima of $\Delta\Lambda_{x(RH)}$ using Gaussian functions in Microcal Origin. Since the maxima of $\Delta\Lambda_{x(CH)}$ are less than 10% of the amplitudes of profiles at comparable energies, the uncertainties in our estimates are large (between 5 and 15 cm^{-1} depending on the spectrum; see Table 2). We have averaged the apparent values of $\Lambda_{x(CH)}$ and $\Lambda_{x(CD)}$ for all complexes except $[Ru(bpy)_3]^{2+}$ in Table 2. The large amplitude noise at $h\nu_x \sim 2500-3500$ cm^{-1} in the spectrum of the latter complex results from noise from the calibration lamp in the 1350−1450 nm range (used for the second-order spectrum of the complex); consequently, we have used the amplitude of the negative peak at about 2800 cm^{-1} to estimate $\Lambda_{x(CH)} = \Lambda_{x(CD)}$ and the uncertainty is correspondingly larger than that for the other complexes. These contributions and the limits that our observations place on the values of the reorganizational energies of the high-frequency vibrational modes are summarized in Table 2.

The contributions of the N−H stretching modes are much smaller and not significantly greater than the limits dictated by the uncertainties in $I_{\nu_m(fit)}$ and the signal-to-noise limits of the spectroscopic experiments (including the detector sensitivity, reproducibility of glass quality, optical alignment, etc.), and our observations can only be used to set upper limits ($\Delta\Lambda_x \leq 5-10$ cm^{-1} for $\nu_x \cong 2800-3200$ cm^{-1}) for those contributions.

Our modeling of the emission spectra based on rR parameters demonstrates that the amplitudes of $\Lambda_{x(C-H)}$ and $\Lambda_{x(N-H)}$ are upper limits and the corresponding vibrational reorganizational energies must be smaller than these quantities by a large factor.[20] We can also set a lower limit for the average of the R−H stretching modes of $(\lambda_{CH})_{ave} \geq 2$ cm^{-1} and $(\lambda_{NH})_{ave} \geq 0.8$ cm^{-1} based on the number (k) of R−H stretches since, for infinite bandwidths (or $\Delta\nu_{1/2}$ much greater than the maximum difference between the C−H stretching frequencies), $\Delta\Lambda_x = \sum_k (\lambda_{RH})_k$. These small amplitude, high-frequency vibronic components would be very difficult to detect in the rR experiments.

Discussion

The perdeuterations of the ligands of the $[Ru(Am)_{6-2n}(bpy)_n]^{2+}$ complexes have significant effects on their emission spectra and lifetimes. The most striking effect is the 2−3 times larger blue shift in $h\nu_{max(f)}$ for the $[Ru(Am)_4bpy]^{2+}$ complexes than for the $[Ru(bpy)_3]^{2+}$ complex on perdeuteration of their bpy ligands (Figure 4). This is qualitatively consistent with the prediction[10] of a greater blue shift when the electron is localized on a single bpy ligand than when it is "delocalized" over three. However, the lack of a detectable blue shift for either the d_5-py or d_8-bpy isotopomers of $[Ru(py)_4bpy]^{2+}$ indicates that a simple "delocalization" mechanism cannot be correct and that several factors must contribute to the emission band origins. Different interpretations of the blue shift have significantly different implications for the properties of the excited state, as, for example, in the kind of mechanisms that should be considered for the excited-state nonradiative relaxation processes. Thus, it is likely that the isotopomeric blue shifts, the differences of ground-state and excited-state vibrational force constants, and the small vibrational reorganizational energies of the C−H and N−H vibrational modes all contribute to the effects of isotopic substitution on the MLCT excited-state lifetimes. However, a very complicated model of the MLCT excited states is required to accommodate these several observations and a quantitative account of the isotope effects remains elusive.

1. Blue Shifts of ∇zpe upon Ligand Perdeuteration: Issues Related to Differences in Vibrational Frequencies. The blue shifts of ∇zpe observed for the CH/CD isotopomers imply smaller force constants of some vibrational modes in the MLCT excited state than in the ground state (GS), consistent with the antibonding character of the bpy LUMO and with the appreciable ligand distortion accompanying the transfer of charge from the metal to the ligand. However, this tendency of bpy skeletal modes to have smaller excited-state force constants will be opposed to some degree by the tendency of the metal−ligand skeletal vibrational modes to be larger for a Ru^{III} center (MLCT excited state) than for a Ru^{II} center (GS).[53] The blue shift of the fundamental of the $[Ru(bpy)_3]^{2+}$ emission in 77 K glasses that results from CH deuteration is $\Delta h\nu_{max(f)} = 30 \pm 10$ cm^{-1}. This agrees to within one standard deviation with the value of 40 cm^{-1} reported for the blue shift of Δzpe in this complex at

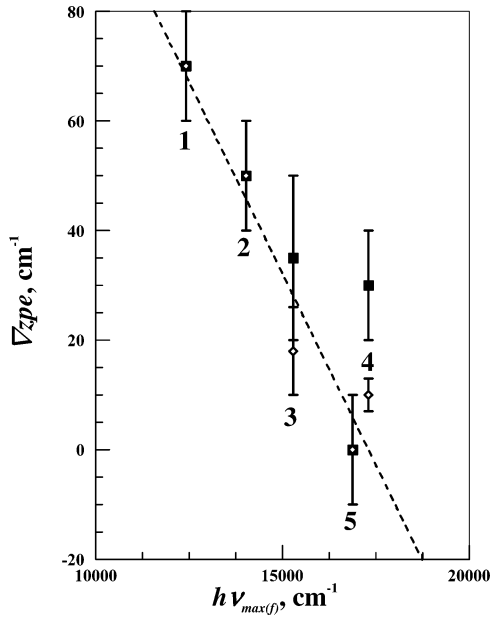

Figure 5. Correlation of the differences of $h\nu_{max(f)}$ for the d_8-bpy and h_8-bpy isotopomers with $h\nu_{max(f)}$ for $[Ru(NH_3)_4bpy]^{2+}$, 1; $[Ru([14]aneN_4)bpy]^{2+}$, 2; $[Ru(en)(bpy)_2]^{2+}$, 3; $[Ru(bpy)_3]^{2+}$, 4; $[Ru(py)_4bpy]^{2+}$, 5. The filled squares are values of ∇zpe from Table 2, and the open diamonds are ∇zpe/*n* (per bpy). Least-squares line (dotted): slope -0.014 ± 0.001 and intercept 242 ± 35 cm^{-1} ($r^2 = 0.92$).

4 K in crystalline solids.[10] The larger blue shifts found for bpy perdeuteration of the $[Ru(Am)_4bpy]^{2+}$ complexes, $\Delta h\nu_{max(f)} = (50 \pm 10)$ to (70 ± 10) cm^{-1}, are qualitatively consistent with the larger value of ∇zpe predicted when the excited-state electron is localized on a single bpy[10] and with some attenuation of the effect as a result of configurational mixing with the ground state. However, Figure 5 indicates that the difference between the fundamental component energies of the emission bands, $\Delta h\nu_{max(f)}$, of the d_8-bpy and h_8-bpy isotopomers increases systematically as $h\nu_{max(f)}$ decreases and the blue shifts observed for the mono-bpy complexes span the full range of the observations. Consequently, there are serious problems with simple interpretations of these variations in the isotopomeric emission band origins: (a) the lack of a significant effect of perdeuteration of either the py or bpy ligands of $[Ru(py)_4bpy]^{2+}$ (Table 2) is very difficult to reconcile with extensive electron delocalization among these ligands; (b) the detailed consideration of the effects of deuteration on the Raman active vibrational modes[14] suggests very complicated contributions to ∇zpe (see below); (c) simple, two-state perturbation theory treatments of the mixing of diabatic ground and excited electronic states are not consistent with the observed trend (section 2 below); (d) the electrochemical properties of the complexes are dominated by mixing with the ground state (section 2 below).

2. Blue Shifts of ∇zpe upon Ligand Perdeuteration: Possible Contributions of Configurational Mixing. The distortions characteristic of the limit in which a full unit of charge is localized on the bpy ligand, $Q = a$ (for a general distortion coordinate such that $Q = 0$ in the GS), will be altered by configurational mixing with the ground state and with electronic excited states. Configurational mixing will tend to reduce the differences in the properties of the ground and excited states, and the effect on variations of $\Delta h\nu_{max(f)}$ can be discussed in terms of the mixing some of the upper state character into the lower state (and vice versa) and this can be expressed in terms of charge delocalization between the configurationally mixed states. In addition, configurational mixing changes the shapes of the PE surfaces, and this will also change the force constants; however, ∇zpe is a function of the difference in vibrational frequencies and consequently of the square roots of the force constants. The general pattern for the changes in shapes of PE surfaces that result from configurational mixing in a two-state limit is that the lowest energy surface will be broadened and the higher energy surfaces will be narrowed (see Figure 1). Opposed to this is the tendency of configurational mixing to average the properties of the two states. Since the force constant is given by the second derivative of PE with respect to the configuration coordinate, the general effects of the changes in shape are to decrease the ground-state force constant and to increase the excited-state force constant. An instructive example is provided by the configurational mixing of the ground state and an excited state with a single distortion mode for which the frequencies in the diabatic limit are $\nu_{g(d)}$ and $\nu_{e(d)}$, respectively, where $\nu_{e(d)} < \nu_{g(d)}$, and for the mixing coefficients at the PE minima with $\alpha_{eg}^2 < \alpha_{ge}^2$. This is qualitatively representative of the effects of mixing any two states on∇zpe, and for the *k*th distortion mode, it can be expressed as

$$(\nabla zpe)_k \approx {}^1/_2\delta_k h\{[\nu_{g(d)}(1 - {}^1/_2\alpha_{ge}{}^2) - \nu_{e(d)}(1 - {}^1/_2\alpha_{eg}{}^2)]\}_k + \delta_k \frac{h}{4}\left\{\nu_{g(d)}\alpha_{ge}{}^2\frac{\lambda_e}{\lambda_g} - \nu_{e(d)}\alpha_{eg}{}^2\frac{\lambda_g}{\lambda_e}\right\}_k \quad (16)$$

See the Appendix and the Supporting Information[26] for further details. In eq 16, δ_k is the average difference in the ratios of the frequencies for the deutereo- and proteo-isotopomer vibrational mode *k* (for a C−H or N−H stretch, $\delta \cong [1 - 2^{-1/2}]$; the isotopomers are assumed to have identical mixing coefficients). The correction terms that have been retained in eq 16 are the simplest consequences of configurational mixing, and none of these terms contributes when $\nu_{e(d)} = \nu_{g(d)}$ and $\alpha_{eg}^2 = \alpha_{ge}^2$. The terms in the first set of braces in eq 16 can be interpreted as the result of averaging the frequencies of the two states, and the terms in the second set of braces can be attributed to the changes of shape of the PE surfaces. Even in the limit that the diabatic excited and ground states have the same force constants and mixing coefficients, there will be terms that contribute to differences in excited-state and ground-state frequencies as a result of the effects of configurational mixing on the shapes of the PE surfaces (e.g., see Figure 1 and eqs 17 and 22). When $\nu_{e(d)} < \nu_{g(d)}$, the increases in α_{eg}^2 and α_{ge}^2 with decreases in $h\nu_{max(f)}$ should decrease the blue shift of the zpe, contrary to our observations.

Thus, while the negative values of ∇zpe imply that some vibrational frequencies of the diabatic excited state are smaller than those of the ground state, and while PE surface distortions expected for excited-state/ground-state configurational mixing (larger for $[Ru(NH_3)_4bpy]^{2+}$ than $[Ru(bpy)_3]^{2+}$) should increase the excited-state frequencies, the frequencies of the ground-state distortion modes reported in the rR spectra of $[Ru(NH_3)_4bpy]^{2+}$ [23] are generally smaller than those of the $[Ru(bpy)_3]^{2+}$ complex.[14] These differences are greater than 10 cm^{-1} for a few vibrational modes: for $[Ru(bpy)_3]^{2+}$ vibrations at 1563, 1491, 1320, 1043, and 283 cm^{-1}, the differences (subtracting $[Ru(NH_3)_4bpy]^{2+}$ frequencies) are $\Delta\nu_k = 15$, 10, −11, 16, and 35 cm^{-1}, respectively. The variations in the frequencies of the ground-state modes with configurational mixing can be expressed as (see the Appendix for more details)

$$\nu_{g(ad)} \approx \nu_{g(d)}\left[1 - \frac{1}{2}\alpha_{ge}{}^2 + \frac{1}{2}\alpha_{ge}{}^2\left(1 - \frac{4\lambda_e}{E_{ge}^{00'} + \lambda_e}\right)\left(\frac{\nu_{e(d)}}{\nu_{g(d)}}\right)^2\right] \quad (17)$$

Thus, the differences in at least some of these frequencies are consistent with (a) $[\nu_{e(d)}/\nu_{g(d)}] < 1$, (b) the averaging of ground-state and excited-state frequencies being a more important result of configurational mixing than are the changes in shape of the PE surfaces, and (c) greater MLCT/GS configurational mixing for the tetraammine complex than for $[Ru(bpy)_3]^{2+}$. If the differences in the frequencies of the ground-state distortion modes that are associated with the bpy ligand (excluding the 1320 and 283 cm^{-1} modes) arise from MLCT/GS configurational mixing, then the observed differences and parameters in Table S1 suggest that these excited-state frequencies differ from those of the ground state in the diabatic limit by approximately 50−500 cm^{-1}. That the observed differences are smaller than these estimates may be the consequence of the opposing effect of the changes of shape in the PE surfaces. However, the uncertainties in the values of $\Delta\nu_k$ are very large so a more quantitative evaluation is not appropriate.

That am(m)ine perdeuteration results in very small or negligible blue shifts of ∇zpe may be a consequence of opposing shifts of the metal−ligand skeletal vibrational modes and the N−H modes: the vibrational frequencies of the former tend to be larger for Ru^{III} than for Ru^{II} while the reverse is the case for the latter.[53] Distortions in both the Ru-bpy and bpy-centered skeletal vibrational modes will contribute to the observed vibronic structure of the emission spectrum, but their effects on ∇zpe will tend to be opposed. The apparently larger blue shift found to result from NH perdeuteration of the diam(m)ine−bis-bpy complexes than of the tetraam(m)ine−mono-bpy complexes may arise from the different combinations of metal−ligand motions that contribute to the normal vibrational modes and the larger contributions of some mode that weights motions along one coordination sphere axis differently from the others; for example, such a motion would be a tetragonal stretch (the t_{2g} stretch in an octahedral complex). That the different charge distributions of the ground and excited state should result in increases in some force constants and decreases in others is not surprising, but it makes the quantitative interpretation of the variations in ∇zpe very difficult.

The smaller ∇zpe found for $[Ru(bpy)_3]^{2+}$ than for $[Ru(NH_3)_4bpy]^{2+}$ might be attributed to smaller force constants for some vibrational modes in the excited state than in the ground state and an effect of configurational mixing between the MLCT excited states that reduces this difference in the former.[10] If this were the case, then perturbation theory arguments indicate that the PE surface of the lowest energy MLCT excited state should be broadened (i.e., smaller force constants) along any distortion coordinate that is correlated with the bpy/bpy^- electron transfer. Consequently, only the vibrational distortion modes that correlate with Ru/bpy electron transfer, but not with bpy/bpy^- electron transfer, could result in a smaller blue shift in ∇zpe for $[Ru(bpy)_3]^{2+}$. The metal−ligand distortion modes might be implicated, and the rR spectra do indicate that the displacements in the Ru−ligand skeletal modes are larger for $[Ru(NH_3)_4bpy]^{2+}$ [23] than for $[Ru(bpy)_3]^{2+}$,[14] consistent with their different contributions to the MLCT excited states of these complexes, but the differences in these modes are not readily attributed to MLCT/MLCT′ mixing. Furthermore, the transfer of charge from the metal is expected to increase the frequencies of most of the metal−ligand vibrational modes, and this is not always the case; for example, the 283 cm^{-1} mode in the $[Ru(bpy)_3]^{2+}$ [14] ground state is apparently shifted to 248 cm^{-1} in $[Ru(NH_3)_4bpy]^{2+}$.[23]

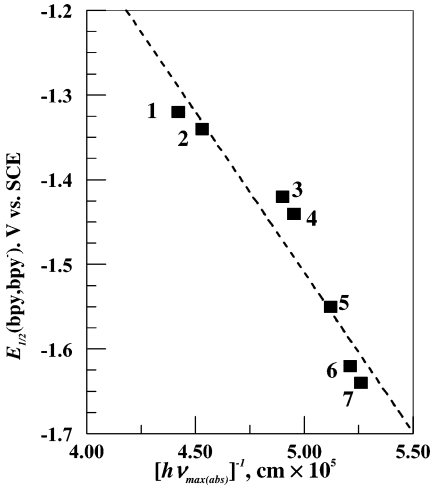

Figure 6. Correlation of the half-wave potential for reduction of bpy in $[Ru(Am)_{2n-6}(bpy)_n]^{2+}$ complexes with the inverse absorption maximum for Am: py, 1; bpy/2, 2; (en, bpy)/4, 3; (NH_3, bpy)/4, 4; ([14]-aneN$_4$)/4, 5; en/2, 6; NH_3, 7. The correlation is based on $E_{1/2}(bpy/bpy^-) = E_{1/2}{}^\circ(bpy/bpy^-) + \epsilon_s \approx H_{ge}{}^2/E_{ge}$. Least-squares line: slope, −0.38 ± 0.05 V cm × 10^5; intercept, 0.4 ± 0.2 V ($r^2 = 0.92$).

If this difference is attributed to the differences in GS/MLCT configurational mixing, then eq 16 implies that the corresponding excited-state vibrational frequency is much smaller, and the observation that the rR spectra frequencies of a metal−ligand skeletal mode are smaller in the excited state may suggest configurational mixing among the excited states, but the implicated states are probably not MLCT excited states.

An additional important consequence of configurational mixing is to decrease the energy of the lowest energy state;[54] see Figure 1. If there were extensive configurational mixing among the MLCT excited states of $[Ru(bpy)_3]^{2+}$, then the LUMO of this complex should have a relatively low energy compared with other complexes in the series. Insofar as the reductions of the $[Ru(Am)_{6-2n}(bpy)_n]^{2+}$ complexes are a measure of LUMO energies,[55] Figure 6 indicates that the variations in these energies are almost entirely attributable to the destabilization ($\epsilon_d \approx \alpha_{ge}{}^2 E_{ge}$) that results from configurational mixing with the ground state[27] and that MLCT/MLCT′ configurational mixing has little effect.

There are low-energy excited states in these complexes, in addition to the MLCT states, that could contribute to aspects of the observed properties and the most obvious of these are (a) a metal-centered, low-energy ligand field excited state ^{3}LF and (b) a ligand-centered $\pi-\pi^*$ excited state. Thus, $[Rh(NH_3)_6]^{3+}$, which is isoelectronic with $[Ru(NH_3)_6]^{2+}$, has a broad emission band centered at about 17 000 cm^{-1} with an origin at about 21 000 cm^{-1}; this emission is assigned to the lowest energy triplet ligand field excited state.[56] Due to the charge difference, the ligand field excited states of Rh^{III} are expected to occur at higher energies than the corresponding states of Ru^{II} and the lowest energy ligand field absorptions of these complexes have their maxima at about 32 500 and 26 500 cm^{-1}, respectively.[56,57] This suggests that the ^{3}LF excited state of $[Ru(NH_3)_6]^{2+}$ should have its origin in the 15 000−17 000 cm^{-1} energy range. The largest energy contributions of the ligand field transitions in these d^6 complexes arise from the differences in the electronic pairing energy and from the energy differences of the dσ and dπ orbitals or $10Dq \cong 3\sigma_L - 4\pi_L$, where σ_L and π_L are the respective orbital energy parameters of the angular overlap model (AOM) determined for the ground-state nuclear coordinates.[57−59] The σ_L parameters are usually approximately the same for the am(m)ine and pyridyl ligands, but the π_L

parameters, usually taken as zero for am(m)ines, are found to be significantly negative for pyridyl ligands.[58,59] Thus, for $[Cr(bpy)_3]^{3+}$, the AOM π_L parameter (per N) has been found to be -250 cm^{-1},[60] and the π_L parameter for $[Ru(bpy)_3]^{2+}$ is expected to have a larger (negative) amplitude. This suggests that the ^{3}LF state energies are only a few thousand wavenumbers larger than the ^{3}MLCT energies and that the ^{3}LF excited-state energies will approximately track the variations of ^{3}MLCT energies in the $[Ru(Am)_{6-2n}(bpy)_n]^{2+}$ complexes. This ^{3}LF excited state is tetragonally distorted (along a e_g configurational coordinate in the octahedral complex),[56] with some relatively weak metal−ligand bonds, and configurational mixing with this state would result in both an increase in the metal−ligand distortion of the ^{3}MLCT excited state and reductions of the corresponding force constants. Such configurational mixing might account for some of the variations in blue shifts and of the vibrational reorganizational energies of the low-frequency distortion modes. Unfortunately, there is no direct experimental information available concerning the energies of the ^{3}LF excited states in these complexes. It may also be relevant that there is an intense absorption in the Ru−bpy complexes at about 34 000 cm^{-1} that is assigned to a $\pi-\pi^*$ transition and that configurational mixing with such local electronic states has been considered to contribute to the intensities of charge-transfer transitions.[54] Thus, configurational mixing with the $\pi-\pi^*$ excited states might also be a factor in the variations of MLCT excited-state force constants.

3. Blue Shifts of ∇zpe upon Ligand Perdeuteration: Implications for Models of Excited-State Properties. The striking differences in the blue shifts of $\Delta h\nu_{max(f)}$ for the CD and CH isotopomers of the $[Ru(py)_4bpy]^{2+}$, $[Ru(bpy)_3]^{2+}$, and $[Ru(NH_3)_4bpy]^{2+}$ complexes demonstrate that their MLCT excited states cannot be described in terms of a simple two-state model involving a single Ru/bpy chromophore and that it is likely that configurational mixing among several of the molecular electronic states must be considered for a useful description of these systems. In addition, the observed ∇zpe's indicate that there are appreciable differences between the ground-state and excited-state force constants for some vibrational modes. For example, δ_k in eq 16 varies from ∼0.02 for the bpy skeletal vibrational modes in the 1491−1608 cm^{-1} range to ∼0.2 for the 1264 and 1043 cm^{-1} modes. [14] Thus, if the zpe's were represented by a single bpy skeletal mode with $\nu_{g(d)} = 1500$ cm^{-1} (equivalent to a single mode representation of the vibronic structure of the emission), then to account for ∇zpe $= 30$ cm^{-1}, $\nu_{e(d)} \sim 100$ cm^{-1} and for ∇zpe $= 70$ cm^{-1}, $\nu_{e(d)} \sim 0$ cm^{-1}. It is obviously more likely that several distortion modes have different (larger or smaller) ground- and excited-state force constants and that the net effect on ∇zpe corresponds to a sum of the terms in eq 16 over all the small contributions of many distortion modes.

It appears that several factors may contribute to the variations in the ∇zpe's and the frequency differences of ground- and excited-state vibrational modes. Thus, the differences in the extent of GS/MLCT configurational mixing through the series of complexes must give rise to some of the variations in the frequencies of the distortion modes such as those found for most of the bpy skeletal modes in the rR spectra[14] since it mixes more of the excited-state character (here, smaller vibrational frequencies) into the ground state as the energy difference between the states decreases, as shown in eq 16; however, Figure 5 suggests that the opposite trend in vibrational frequencies is dominant in the variations in ∇zpe. Several lines of evidence suggest that an important factor contributing to the latter is configurational mixing between the ^{3}MLCT excited state and a slightly higher energy ^{3}LF excited state.

4. Contributions of the High-Frequency C−H and N−H Stretching Modes. The isotopomer emrep's indicate that the vibrational reorganizational energies are very small for the C−H and N−H stretching modes. Since the Λ_x amplitudes are always larger than the amplitudes of the vibrational reorganizational energy components when $\Delta\nu_{1/2}$ is comparable to or greater than the differences in the vibrational energies of several distortion modes,[20] and since there are 8 C−H stretching modes in bpy and 12 N−H stretching modes in the tetraammine, the observed Λ_{CH} and Λ_{NH} amplitudes are greater than the amplitudes of any of the respective vibrational reorganizational energies but smaller than the sum of the individual λ_{RH} amplitudes of all of the C−H or N−H stretching modes, respectively. Thus, for the average of the vibrational reorganizational energies amplitudes: $25 > (\lambda_{CH(av)})/\text{cm}^{-1} > 3$ and $5 \gg (\lambda_{NH(av)})/\text{cm}^{-1} \geq 0$. The estimates of Λ_{CH} are significantly larger for $[Ru(bpy)_3]^{2+}$ than for $[Ru(Am)_4bpy]^{2+}$ consistent with the attenuation expected on the basis of eq 15. The very small displacements implied by the values for Λ_{RH} indicate that the high-frequency C−H and N−H stretching modes do not contribute significantly to the MLCT excited-state properties.

5. Kinetic Isotope Effects on MLCT Excited-State Lifetimes. Most models for excited-state nonradiative relaxation assume that the force constants of the ground and excited state are the same.[5,21,22,61,62] The ∇zpe's found in this study and the above discussion indicate that this is not the case for the $[Ru(NH_3)_{6-2n}(bpy)_n]^{2+}$ complexes, and the differences may be very large for some of the vibrational modes, especially since it appears that the force constants increase for some modes in the excited state while for others they decrease. Consequently, models that assume identical force constants cannot be correct. In addition, the use of the observed values of Λ_{RH} (or estimates of $\lambda_{RH} < \Lambda_{RH}$), which is equivalent to the use of a single distortion mode model in a typical rate constant expression for nuclear tunneling[21]

$$k_{nr} = A \exp\left(-\gamma_x \frac{E_{max(f)}}{h\nu_x}\right)$$
$$\gamma_x = \ln(E_{max(f)}/\Lambda_x) - 1 \qquad (18)$$

underestimates the relaxation rate constant by 4−9 orders of magnitude, depending on the complex and assumptions about A, and it overestimates the isotope effect (see also the previous discussions of these issues).[15,20] Nevertheless, there are some important implications of these observations.

If the high-frequency C−H and N−H vibrational modes made the predominant contributions to the MLCT excited-state relaxation channels, then one would expect the effect of perdeuteration to be largest for the high-frequency modes with the largest vibrational reorganizational energies; that is, since $\Lambda_{CH} > \Lambda_{NH}$, one would expect a larger isotope effect for bpy than for am(m)ine perdeuteration. That the opposite order is observed is evidence that these vibrational modes are not major contributors to excited-state relaxation; nevertheless, some contribution is possible in combination with other vibrational modes. Thus, Kincaid and co-workers have rationalized the different lifetimes of the isotopomers of $[Ru(bpy)_3]^{2+}$ in terms of the combined second-order effects of CH/CD substitution on the bpy skeletal modes.[14] Since the isoenergetic crossing from the MLCT excited state into such relaxation channels of the ground state corresponds to at least 7 quanta of excitation in the bpy ligand skeletal vibrational modes and since a large number of distortion modes are implicated by the high-resolution, low-temperature spectroscopy[9,10] and by the rR spectroscopy,[14,23] there are vast number of different relaxation

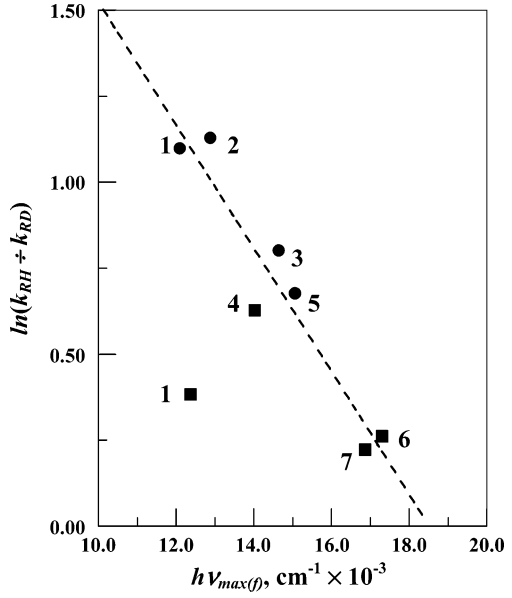

Figure 7. Correlation of $\ln(k_{RH}/k_{RD})$ with $h\nu_{max(f)}$ for R = C in butyronitrile (filled squares): $[Ru(NH_3)_4bpy]^{2+}$, 1; $[Ru([14]aneN_4)bpy]^{2+}$, 4; $[Ru(bpy)_3]^{2+}$, 6; $[Ru(py)_4bpy]^{2+}$, 7. For R = N: $[Ru(NH_3)_4bpy]^{2+}$, 1; $[Ru(en)_2bpy]^{2+}$, 2; $[Ru(NH_3)_2(bpy)_2]^{2+}$, 3; $[Ru(en)(bpy)_2]^{2+}$, 5. Least squares line (dashed; omitting the point for $[Ru(NH_3)_4(d_8\text{-bpy})]^{2+}$): slope, 00.77 ± 0.02 cm^{-1} × 10^3; intercept, 3.3 ± 0.4 (r^2 = 0.91).

channels, each composed of a different combination of these distortion modes. Consequently, it is likely that some vibrational modes with larger quanta but smaller reorganizational energies are incorporated into some of these relaxation channels. In this regard, it is interesting that k_{NH}/k_{ND} is approximately proportional to the number of NH moieties while Λ_{NH} is very close to zero and that, except for $[Ru(NH_3)_4(d_8\text{-bpy})]^{2+}$, the observed isotope effects decrease exponentially with an increasing excited-state−ground-state energy difference (see Figure 7).

Since am(m)ine perdeuteration will not have a significant effect on the vibrational frequencies of the bpy ligand, the substantial isotope effects, together with the issues related to the∇zpe's discussed above, implicate contributions of some of the low-frequency Ru-am(m)ine skeletal vibrations and possibly also contributions of the NH vibrational modes in a significant number of the relaxation channels, even though the former have very small vibrational quanta and the latter have very small vibrational reorganizational energies.

Conclusions

Perdeuteration of the bpy ligand in $[Ru(Am)_{6-2n}(bpy)_n]^{2+}$ complexes results in much larger blue shifts of the emission fundamental when $n = 1$ than when $n = 3$, qualitatively in agreement with the prediction of Yersin.[10] However, perdeuteration of the ligands of $[Ru(py)_4bpy]^{2+}$ does not result in a measurable shift of the emission maximum or of $h\nu_{max(f)}$.

In contrast to the shifts observed in the same complexes following perdeuteration of bpy, the perdeuteration of coordinated am(m)ines leads to small or no blue shifts in ∇zpe in this group of complexes and this suggests that there is a cancellation of the effects of vibrational modes whose force constants are larger (associated with oxidation of the Ru donor) in the excited state and those whose force constants are smaller. Some of this complexity probably arises from different extents of configurational mixing among the excited states of these complexes, for example, it is likely that configurational mixing with a low-energy ^{3}LF excited state is an important factor in the variations of the observed parameters.

The careful comparison of emission spectra of the isotopomers has permitted the resolution of very small in amplitude C−H vibronic components. In contrast, the N−H vibronic contributions to the emission spectrum are too weak to resolve (λ_{NH} is probably less than 2 cm^{-1} for the N−H stretching modes of the $[Ru(NH_3)_4bpy]^{2+}$ complex). Such small vibrational reorganizational energies lead to very small contributions of the highest frequency vibrational modes to the excited-state relaxation rates in single mode/single relaxation channel models, and this suggests that the lifetimes of this series of complexes are determined by the following: (1) the sum of the very small contributions of a very large number of excited state relaxation channels, each corresponding to the population vibrations that are combinations of a large number of generally different ground-state modes and (2) factors related to the differences between the ground-state and excited-state force constants.

Acknowledgment. The authors thank the Office of Basic Energy Sciences of the Department of Energy for partial support of this research. We are also grateful to Professor James R. Kincaid for helping to initiate this study by providing us with a sample of $[Ru(d_8\text{-bpy})_3]^{2+}$.

Appendix

Effect of MLCT/GS Configurational Mixing on the Force Constant and the Zero-Point Energy. Configurational mixing will tend to mix the ground- and the excited-state force constants, and a single mode argument[26] is useful to illustrate the effects of configurational mixing. The effects of configurational mixing on vibrational frequencies, and thereby on zpe's, can be interpreted in terms of changes in the distribution of electron density and/or changes in the shapes of the PE surfaces. These issues are most readily addressed in terms of the effective force constants since in the sho limit the second derivative of the PE function, evaluated at the PE minimum, is equal to the force constant. Thus, for a two-state system initially assume that the distortion is in a single vibrational mode with a ground-state force constant f_g and an excited-state force constant f_e, a nuclear coordinate $Q = 0$ for the ground-state PE minimum and $Q = a$ for the excited-state PE minimum, and $E_{ge}^{0'0}$ the zero-point energy difference between the excited- and ground-state PE minima. Then $V_g^\circ = {}^1/_2 f_{g(d)} Q^2$ and $V_e^\circ = {}^1/_2 f_{e(d)}(Q - a)^2 + E_{ge}^{0'0}$ (the subscript d designates parameters before configurational mixing). It is convenient to define the respective vibrational reorganizational energies as $\lambda_g = {}^1/_2 f_{g(d)} a^2$ and $\lambda_e = {}^1/_2 f_{e(d)} a^2$, and a reduced coordinate $q = Q/a$, so that the adiabatic PEs are[26]

$$V_g = \lambda_g q^2 + \epsilon_-$$

and

$$V_e = \lambda_g q^2 + \epsilon_+ \qquad (19)$$

where $\epsilon_\pm = {}^1/_2 \xi \pm {}^1/_2[\xi^2 + 4h^2]^{1/2}$ and $\xi = V_e^\circ - V_g^\circ = \Delta\lambda q^2 - 2\lambda_e q + \lambda_e + E_{ge}^{0'0}$. Then, for α_{ge}^2 and α_{eg}^2 less than 0.1 and $E_{ge}^{0'0} \gg (H_{ge}, \lambda_g, \text{or } \lambda_e)$[26]

$$f_{g(ad)} \approx f_{g(d)}(1 - \alpha_{ge}^2) + \alpha_{ge}^2 f_{e(d)} - \frac{4\alpha_{ge}^2 \lambda_e}{E_{ge}^{0'0} + \lambda_e} f_{e(d)} + \ldots \quad (20)$$

$$f_{e(ad)} \approx f_{e(d)}(1 - \alpha_{eg}^2) + \alpha_{eg}^2 f_{g(d)} + \frac{4\alpha_{eg}^2 \lambda_g}{E_{ge}^{0'0} - \lambda_g} f_{g(d)} + \ldots \quad (21)$$

Since the emission is nominally a triplet−singlet transition, one expects that $\alpha_{eg}^2 < \alpha_{eg}^2$ and $\alpha_{eg}^2 < \alpha_{ge}^2(\nu_{g(d)}^2/\nu_{e(d)}^2)$, so for $f_i = 4\pi\mu_m\nu_i^2$ (μ_m = reduced mass) and $(\nu_{g(d)}/\nu_{e(d)})^2 = f_{g(d)}/f_{e(d)} = \lambda_g/\lambda_e$, the altered vibrational frequencies are given by eq 17 and

$$\nu_{e(ad)} \approx \nu_{e(d)}\left[1 - \frac{1}{2}\alpha_{eg}^2 + \frac{1}{2}\alpha_{eg}^2\left(1 + \frac{4\lambda_g}{E_{ge}^{00'} - \lambda_g}\right)\left(\frac{\nu_{g(d)}}{\nu_{e(d)}}\right)^2\right]$$

$$\approx \nu_{e(d)}\left[1 - \frac{1}{2}\alpha_{eg}^2 + \frac{1}{2}\alpha_{eg}^2\frac{\lambda_g}{\lambda_e}\right] \quad (22)$$

The single mode (k) contribution to the zpe difference for the isotopomers is

$$(\nabla zpe)_k = {}^1/_2h[\nu_{g(ad)} - \nu_{e(ad)}]_{RD} - {}^1/_2h[\nu_{g(ad)} - \nu_{e(ad)}]_{RH} \quad (23)$$

so that for $\nu_{e(d)} < \nu_{g(d)}$ and $\alpha_{eg}^2 < \alpha_{ge}^2$, one obtains eq 16.

Even when the diabatic excited and ground states have the same force constants and mixing coefficients, the $\alpha_{jk}^2(4\lambda_k/E_{jk}^{00'} - \lambda_k)$ terms in eqs 17 and 22 will contribute to differences in excited-state and ground-state frequencies as a result of the effects of configurational mixing on the shapes of the PE surfaces (e.g., see Figure 1).

Supporting Information Available: Tables of attenuation parameters, figures of spectroscopic data and bandwidth dependence of $h\nu_{max(f)}$, and perturbation theory details. This material is available free of charge via the Internet at http://pubs.acs.org.

References and Notes

(1) Juris, A.; Balzani, V.; Barigelletti, F.; Compagna, S.; Belser, P. l.; von Zelewsky, A. *Coord. Chem. Rev.* **1988**, *84*, 85.

(2) Kalyanasundaram, K. *Photochemistry of Polypyridine and Porphyrin Complexes*; Academic Press: New York, 1992.

(3) Kober, E. M.; Casper, J. V.; Lumpkin, R. S.; Meyer, T. J. *J. Phys. Chem.* **1986**, *90*, 3722.

(4) Meyer, T. J. *Prog. Inorg. Chem.* **1983**, *30*, 389.

(5) Barbara, P. F.; Meyer, T. J.; Ratner, M. *J. Phys. Chem.* **1996**, *100*, 13148.

(6) Graff, D.; Claude, J. P.; Meyer, T. J. In *Electron-Transfer Reactions: Inorganic, Organometallic and Biological Applications*; Isied, S. S., Ed.; American Chemical Society: Washington, DC, 1997; p 183.

(7) Endicott, J. F.; Chen, Y.-J.; Xie, P. *Coord. Chem. Rev.* **2005**, *249*, 343.

(8) Krausz, E.; Ferguson, J. *Prog. Inorg. Chem.* **1989**, *37*, 293.

(9) Yersin, H.; Braun, D.; Hensler, G.; Galhuber, E. In *Vibronic Processes in Inorganic Chemistry*; Flint, C. D., Ed.; Kluwer: Dordrecht, The Netherlands, 1989; p 195.

(10) Yersin, H.; Braun, D. *Chem. Phys. Lett.* **1991**, *179*, 85.

(11) Riesen, H.; Krausz, E. *Comments Inorg. Chem.* **1995**, *18*, 27.

(12) Browne, W. R.; Vos, J. G. *Coord. Chem. Rev.* **2001**, *219*−*221*, 761.

(13) Yersin, H.; Humbs, W.; Strasser, J. *Coord. Chem. Rev.* **1997**, *159*, 325.

(14) Maruszewski, K.; Bajdor, K.; Strommen, D. P.; Kincaid, J. R. *J. Phys. Chem.* **1995**, *99*, 6286.

(15) Chen, Y.-J.; Xie, P.; Endicott, J. F. *J. Phys. Chem. A* **2004**, *108*, 5041.

(16) Browne, W. R.; O'Boyle, N. M.; Henry, W.; Gluckian, A. L.; Horn, S.; Fett, T.; O'Connor, C. M.; M., D.; De Cola, L.; Coates, C. G.; Ronayne, K. L.; McGarvey, J. J.; Vos, J. G. *J. Am. Chem. Soc.* **2005**, *127*, 1229.

(17) Krausz, E.; Riesen, H. *Coord. Chem. Rev.* **1997**, *159*, 9.

(18) Van Houten, J.; Watts, R. J. *J. Am. Chem. Soc.* **1975**, *97*, 3843.

(19) Liu, F.; Meyer, G. J. *J. Am. Chem. Soc.* **2005**, *127*, 824.

(20) Xie, P.; Chen, Y.-J.; Uddin, M. J.; Endicott, J. F. *J. Phys. Chem. A* **2005**, *109*, 4671.

(21) Englman, R.; Jortner, J. *Mol. Phys.* **1970**, *18*, 145.

(22) Freed, K. F.; Jortner, J. *J. Chem. Phys.* **1970**, *52*, 6272.

(23) Hupp, J. T.; Williams, R. T. *Acc. Chem. Res.* **2001**, *34*, 808.

(24) Xie, P.; Chen, Y.-J.; Endicott, J. F.; Uddin, M. J.; Seneviratne, D.; McNamara, P. G. *Inorg. Chem.* **2003**, *42*, 5040.

(25) Chen, Y.-J.; Endicott, J. F.; Swayambunathan, V. *Chem. Phys.*, in press.

(26) Supporting Information.

(27) Seneviratne, D. S.; Uddin, M. J.; Swayambunathan, V.; Schlegel, H. B.; Endicott, J. F. *Inorg. Chem.* **2002**, *41*, 1502.

(28) Coe, B. J.; Harris, J. A.; Brunschwig, B. S.; I., A.; Clays, K.; Garin, J.; Orduna, J. *J. Am. Chem. Soc.* **2005**, *127*, 13399.

(29) Barefied, E. K.; Wagner, F.; Herlinger, A. W.; Dahl, A. R. *Inorg. Synth.* **1976**, *16*, 221.

(30) Dixon, N. E.; Lawrence, A.; Lay, P. A.; Sargeson, A. M.; Taube, H. *Inorg Synth.* **1986**, *24*, 243.

(31) Callahan, R. W.; Brown, G. M.; Meyer, T. J. *Inorg. Chem.* **1975**, *14*, 1443.

(32) Brown, G. M.; Sutin, N. *J. Am. Chem. Soc.* **1979**, *101*, 883.

(33) Brown, G. M.; Kreutzian, H. J.; Abe, M.; Taube, H. *Inorg. Chem.* **1979**, *18*, 3374.

(34) Krause, R. A. *Inorg. Chim. Acta* **1977**, *22*, 209.

(35) Bryant, G. M.; Ferguson, J. E.; Powell, H. K. *Aust. J. Chem.* **1971**, *24*, 257.

(36) Sakai, K.; Yamada, Y.; Tsubomura, T. *Inorg. Chem.* **1996**, *35*, 3163.

(37) Ryu, C. K.; Lessard, R. B.; Lynch, D.; Endicott, J. F. *J. Phys. Chem.* **1989**, *93*, 1752.

(38) Lessard, R. B.; Endicott, J. F.; Perkovic, M. W.; Ochrymowycz, L. A. *Inorg. Chem.* **1989**, *28*, 2574.

(39) Myers, A. B. *Chem. Rev.* **1996**, *96*, 911.

(40) Myers, A. B. *Acc. Chem. Res.* **1998**, *30*, 5519.

(41) Gould, I. R.; Noukakis, D.; Gomez-Jahn, L.; Young, R. H.; Goodman, J. L.; Farid, S. *Chem. Phys.* **1993**, *176*, 439.

(42) Myers, A. B. In *Laser Techniques in Chemistry*; Myers, A. B., Rizzo, T. R., Eds.; John Wiley & Sons: New York, 1995; Vol. XXIII; p 325.

(43) Yardley, J. T. *Introduction to Molecular Energy Transfer*; Academic: New York, 1980.

(44) Seneviratne, D. S.; Uddin, M. J.; Swayambunathan, V.; Schlegel, H. B.; Endicott, J. F. *Inorg. Chem.* **2002**, *41*, 1502.

(45) Endicott, J. F. In *Electron Transfer in Chemistry*; Balzani, V., Ed.; Wiley-VCH: New York, 2001; Vol. 1, p 238.

(46) Endicott, J. F. In *Comprehensive Coordination Chemistry II*, 2nd ed.; McCleverty, J., Meyer, T. J., Eds.; Pergamon: Oxford, U.K., 2003; Vol. 7, p 657.

(47) Solomon, E. I. *Comments Inorg. Chem.* **1984**, *3*, 225.

(48) Brunold, T. C.; Gudel, H. U. In *Inorganic Electronic Structure and Spectroscopy*; Solomon, E. I., Lever, A. B. P., Eds.; Wiley-Interscience: New York, 1999; Vol. 1, p 259.

(49) Matyushov, D. V.; Voth, G. A. *J. Phys. Chem. A* **2000**, *104*, 6470.

(50) Matyushov, D. V.; Newton, M. D. *J. Phys. Chem. A* **2001**, *105*, 8516.

(51) Endicott, J. F.; Uddin, M. J.; Schlegel, H. B. *Res. Chem. Intermed.* **2002**, *28*, 761.

(52) Strukl, J. S.; Walter, J. L. *Spectrochim. Acta, Part A* **1971**, *27*, 209.

(53) Nakamoto, K. *Infrared and Raman Spectra of Inorganic and Coordination Compounds. Part B*; Wiley: New York, 1997.

(54) Mulliken, R. S.; Person, W. B. *Molecular Complexes*; Wiley-Interscience: New York, 1967.

(55) Lever, A. B. P.; Dodsworth, E. In *Electronic Structure and Spectroscopy of Inorganic Compounds*; Lever, A. B. P., Solomon, E. I., Eds.; Wiley: New York, 1999; Vol. II, p 227.

(56) Hakamata, K.; Urushiyama, A.; Kupka, H. *J. Phys. Chem.* **1981**, *85*, 1983.

(57) Lever, A. B. P. *Inorganic Electronic Spectroscopy*; Elsevier: Amsterdam, The Netherlands, 1984.

(58) Figgis, B. N.; Hitchman, M. A. *Ligand Field Theory and its Applications*; Wiley-VCH: New York, 2000.

(59) Vanquickenbourne, L. G.; Ceulemans, A. *Coord. Chem. Rev.* **1983**, *100*, 157.

(60) Ryu, C. K.; Endicott, J. F. *Inorg. Chem.* **1987**, *27*, 2203.

(61) Birks, J. B. *Photophysics of Aromatic Molecules*; Wiley-Interscience: New York, 1970.

(62) Bixon, M.; Jortner, J.; Cortes, J.; Heitele, H.; Michel-Beyerle, M. E. *J. Phys. Chem.* **1994**, *98*, 7289.